Available online at www.sciencedirect.com

ScienceDirect

IFAC Papers Online CONFERENCE PAPER ARCHIVE

IFAC PapersOnLine 56-2 (2023) 11273–11280

A Constrained Control Allocation and Tuning Scheme for Hybrid Actuators in Spacecraft Attitude Control [1]

Mariusz E. Grøtte * **J. Tommy Gravdahl** * **Tor A. Johansen** *

* *Center for Autonomous Marine Operations and Systems (AMOS), Department of Engineering Cybernetics, Norwegian University of Science and Technology, Trondheim 7034, Norway (e-mail: {mariusz.eivind.grotte, jan.tommy.gravdahl, tor.arne.johansen }@ntnu.no).*

Abstract: Agile rotational maneuvers of spacecraft requires careful execution since its actuators may not be able to produce the demanded torques, causing the state trajectories to deviate and a desired attitude would not be guaranteed. We investigate the control allocation problem for a redundant set of hybrid actuators that include reaction wheels, magnetorquers, and continuous-force thrusters. The main objective of the magnetorquers is to dump momentum from the reaction wheels, whereas the wheels are the primary actuators in attitude control, and more agile maneuvers or faster unloading of momentum can be handled by the thrusters. A modified mixed optimization scheme for control allocation is presented where the equality constraints account for satisfying the high-level (virtual) control inputs for both attitude control and momentum dumping. Variants of dynamic weights in the optimization are developed such that magnetorquers and thrusters may contribute with a relative degree of importance in the attitude control problem. The control allocation scheme is solved using quadratic programming where simulation results are shown for fast and slow rotational maneuvers together with fast and slow momentum dumping.

Copyright © 2023 The Authors. This is an open access article under the CC BY-NC-ND license (https://creativecommons.org/licenses/by-nc-nd/4.0/)

Keywords: aerospace; optimization; rigid body; control allocation

1. INTRODUCTION

Fast and large spacecraft maneuvers require significant amount of torques which may risk the actuators operating at their saturation limits, causing potential damage and fatigue. Minimum-time maneuvers have been investigated for rigid body spacecraft (Bilimoria and Wie, 1993; Scrivener and Thompson, 1994; Steyn, 1995; Fleming et al., 2010; Melton, 2014; Sin et al., 2021), and maneuvers where minimizing fuel and/or time (energy), with e.g. bang-off-bang control profiles, have also been studied for spacecraft rigid bodies (Seywald et al., 1994; Liu and Singh, 1997), but these define the high-level control inputs as a preliminary design step should obtain the actual torques from available actuators.

Control allocation (CA) for real-time implementation has been a widely studied topic, being applicable for many systems such as automobiles, marine vessels, aircraft and spacecraft (Johansen and Fossen, 2013; Bodson, 2002; Oppenheimer et al., 2006; Harkegard, 2002). Static actuation models may in theory be used for any attitude control problems involving large open-loop rotational maneuvers or small attitude corrections (e.g. pointing). For CA design with constraints in terms of actuator rates, then dynamic actuator models may be preferred (Johansen and Fossen, 2013).

We investigate CA for a spacecraft with a redundant set of hybrid actuators for attitude control. The acuators consist of a configuration of reaction wheels and magnetorquers, and, in addition, thrusters which enable faster time to orient the spacecraft. Otherwise, such fast maneuvers may demand significant torques and quickly saturate the other actuators, e.g., in an abrupt event such as immediate stabilization after space debris collision or highly transient events that must be observed and tracked by a sensor. Typically, the magnetorquers are dedicated to dumping momentum from the reaction wheels that accumulate under secular external torque perturbations, enabling the wheels to eventually operate within safer margins from speed dead-zones and saturation limits. However, the efficiency of magnetorquers can be compromised if the surrounding magnetic field is weak (e.g., at apogee in an highly elliptical orbit) or when it is non-existing. Faster actuators, such as coupled thrusters, can help to mitigate this but at the cost of expendable energy. Instead of solving the control problem(s) separately with only one group/type of actuators at a time, we seek to include all actuators in one optimization framework that minimizes control effort in a prioritized manner. The main contributions in this paper are: 1) formalization of constraints in standard quadratic pro-

[1] This work was supported by the Research Council of Norway, Equinor, Det Norske Veritas (DNV) and Sintef through the Centers of Excellence funding scheme, Grant 223254—Center for Autonomous Marine Operations and Systems (AMOS) and the Research Council of Norway through the IKTPLUSS programme grant 270959 (MASSIVE).

2405-8963 Copyright © 2023 The Authors. This is an open access article under the CC BY-NC-ND license.
Peer review under responsibility of International Federation of Automatic Control.
10.1016/j.ifacol.2023.10.321

gramming (QP) to include error minimization objectives for both attitude control and reaction wheel momentum dumping; 2) introducing variants of dynamic weights for the magnetorquers and thrusters that take into account the environmental magnetic field and the importance of errors in momentum and attitude.

This paper is organized as follows. Section 2 describes the attitude representation, the dynamics for an internally and externally actuated spacecraft, and the chosen actuators and their main functions. Section 3 describes the constrained CA using QP to obtain optimized distribution of controls, and the selection of dynamic weights for better use of each actuator type. Finally, results are presented in Section 4 and conclusions are given in Section 5.

1.1 Preliminaries

The ℓ_2 norm of a vector $\mathbf{a} = [x_1,\, x_2,\, \ldots,\, x_n]^\intercal \in \mathbb{R}^n$ is $\|\mathbf{a}\| \triangleq \|\mathbf{a}\|_2 = (\mathbf{a}^\intercal\mathbf{a})^{1/2}$. A unit vector is denoted by $\hat{\mathbf{a}} = \mathbf{a}/\|\mathbf{a}\|$. The square identity matrix and matrix of zeros are denoted by $\mathbf{I}_n \in \mathbb{R}^{n\times n}$ and $\mathbf{0}_{n\times m} \in \mathbb{R}^{n\times m}$, respectively. Let $\mathbf{a} \in \mathbb{R}^3$, then the cross product operator is a 3×3 skew-symmetric matrix,

$$[\mathbf{a}\times] = -\,[\mathbf{a}\times]^\intercal \triangleq \begin{bmatrix} 0 & -a_3 & a_2 \\ a_3 & 0 & -a_1 \\ -a_2 & a_1 & 0 \end{bmatrix}.$$

Functions $f(\cdot)$ of time $t \in \mathbb{R}$ are denoted by $f(t)$ when necessary to highlight its time-dependency, otherwise the time-dependency is not shown.

2. MODEL

For a torque input $\boldsymbol{\tau} \in \mathbb{R}^3$, the attitude and gyrostat equations of motion for a rigid body spacecraft, expressed in body frame coordinates, are

$$\dot{\mathbf{q}} = \frac{1}{2}\begin{bmatrix} -\mathbf{q}_v^\intercal \\ q_0\mathbf{I}_3 + [\mathbf{q}_v]_\times \end{bmatrix}\boldsymbol{\omega}, \tag{1a}$$

$$\mathbf{J}\dot{\boldsymbol{\omega}} = -\,[\boldsymbol{\omega}\times]\,\mathbf{h} + \boldsymbol{\tau} + \boldsymbol{\tau}_h + \mathbf{d}, \tag{1b}$$

where $\mathbf{q} = [q_0,\, \mathbf{q}_v^\intercal]^\intercal$, with $q_0 \in \mathbb{R}$ and $\mathbf{q}_v \in \mathbb{R}^3$, is the unit quaternion satisfying the constraint $q_0^2 + \mathbf{q}_v^\intercal\mathbf{q}_v = 1$; $\boldsymbol{\omega}$ is the angular velocity of the spacecraft body frame relative to an inertial frame; $\boldsymbol{\tau}_h \in \mathbb{R}^3$ is another secondary torque input; $\mathbf{d} \in \mathbb{R}^3$ is a disturbance torque vector; $\mathbf{J} \in \mathbb{R}^{3\times 3}$ is the symmetric inertia matrix of the total system; and $\mathbf{h} \in \mathbb{R}^3$ is the angular momentum of the total system. Attitude errors are defined as $\mathbf{q}_e = \mathbf{q}^{-1} \otimes \mathbf{q}_d$ where $\mathbf{q}^{-1} = \overline{\mathbf{q}}/\|\mathbf{q}\|$ with $\mathbf{q}_d$ being the desired quaternion, $\overline{\mathbf{q}} = [q_0,\, -\mathbf{q}_v^\intercal]^\intercal$ is the quaternion conjugate, and $\otimes$ is the quaternion product; and $\boldsymbol{\omega}_e = \boldsymbol{\omega} - \boldsymbol{\omega}_d$ is the angular velocity error for a desired angular velocity $\boldsymbol{\omega}_d$.

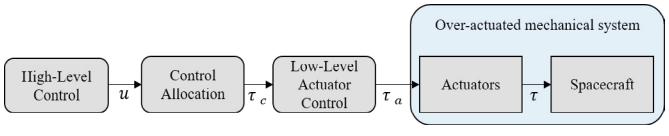

Fig. 1. Mapping of the control input $\mathbf{u}$ to actual torque $\boldsymbol{\tau}$ in the system (1b) through CA.

For the system with p actuators and 3 degrees of freedom, a main virtual control input $\mathbf{u} \in \mathbb{R}^3$ obtained by a high-level controller is, as shown in Fig. (1), mapped to the actual control torque $\boldsymbol{\tau}$ by

$$\mathbf{u}(t) = \boldsymbol{\tau}(t) = \mathbf{C}(t)\boldsymbol{\tau}_c(t) = \mathbf{C}(t)\mathbf{E}(t)\boldsymbol{\tau}_a(t), \tag{2}$$

where $\mathbf{C}(t) \in \mathbb{R}^{3\times p}$ is a matrix of distribution coefficients that are time-varying in general, $\boldsymbol{\tau}_c \in \mathbb{R}^p$ are the commanded control torques to the individual actuators, $\boldsymbol{\tau}_a$ is the vector of actual control efforts produced by the actuators that belong to the set $\mathcal{T}_a = \{\boldsymbol{\tau}_a \in \mathbb{R}^p | \underline{\boldsymbol{\tau}}_a \le \boldsymbol{\tau}_a \le \overline{\boldsymbol{\tau}}_a\}$ for lower limit $\underline{\boldsymbol{\tau}}_a$ and upper limit $\overline{\boldsymbol{\tau}}_a$, and $\mathbf{E} \in \mathbb{R}^{p\times p}$ is an effectiveness matrix. With $p > 3$, the assembly of actuators is redundant (overactuated) and a solution to (2) is non-unique as the inverse $\mathbf{C}^{-1}$ does not exist. The purpose of a general CA scheme is to obtain a solution $\boldsymbol{\tau}_c$ that satisfies the equality in (2), with secondary objective being to minimize the control effort in the set of admissible controls constrained by, e.g., saturation limits and/or singularities.

The efficiency matrix is assumed to be $\mathbf{E} = \mathbf{I}_p$ for all time t, i.e. there is no faults nor efficiency degradation of the actuators. Therefore, $\boldsymbol{\tau}_c \equiv \boldsymbol{\tau}_a$. Further discussion on this can be found in (Hu et al., 2018; Cristofaro and Johansen, 2014), where CA schemes account for failures and degraded efficiencies can be detected and monitored.

2.1 Actuators

Here the spacecraft is taken to be equipped with three types of actuators that can be grouped in hierarchy according to the degree of torque demand:

(1) Slow actuators, e.g., magnetorquers, for smaller degree of attitude control and possibly unloading secular momentum built up in the reaction wheels, operating at full duty cycle when possible;
(2) Main actuators, e.g. reaction wheels, for attitude control and stabilization, nominally operating at full duty cycle;
(3) Fast actuators, e.g., thrusters or CMGs, for agile rotational maneuvers, which, due to significant power/fuel consumption, are only used when no other option is available. Continuous-force thrusters in static configuration are assumed here. Using CMGs as fast actuators for attitude control, then the geometric configuration is in general time-varying, see (Leeghim and Kim, 2021; Hu and Tan, 2020) for further information about including CMGs in CA.

Let the actual control effort be $\boldsymbol{\tau}_a = [\boldsymbol{\tau}_w^\intercal,\, \mathbf{m}^\intercal,\, \boldsymbol{\tau}_T^\intercal]^\intercal \in \mathbb{R}^p$, where $\boldsymbol{\tau}_w \in \mathbb{R}^r$, and $\boldsymbol{\tau}_T \in \mathbb{R}^k$ are torques produced by reaction wheels and fast actuators, respectively, and $\mathbf{m} \in \mathbb{R}^l$ are magnetic dipole moments produced by the magnetorquers. For instance, without a surrounding magnetic field, any powered magnetorquers should be shut down as they may interact with spacecraft electronics and create unwanted disturbance torques. In general, the distribution matrix may be partitioned into block matrices,

$$\mathbf{C} = [-\mathbf{C}_w,\, \theta\mathbf{C}_m(t),\, \mathbf{C}_T] \tag{3}$$

where $\mathbf{C}_w \in \mathbb{R}^{3\times r}$, $\mathbf{C}_m \in \mathbb{R}^{3\times l}$, and $\mathbf{C}_T \in \mathbb{R}^{3\times k}$ relate to reaction wheels, magnetorquers, and fast actuators, respectively, and the parameter $\theta \in \mathbb{R}$ is a piecewise constant switching parameter,

$$\theta = \begin{cases} 1, & \text{if} \quad \|\mathbf{b}\| > \epsilon, \\ 0, & \text{if} \quad \|\mathbf{b}\| \le \epsilon, \end{cases} \tag{4}$$

for some constant $\epsilon > 0$ and $\mathbf{b} \in \mathbb{R}^3$ is the strength of a local external magnetic field. The distribution of magnetic moments are mapped to torques in the body frame by

$$\mathbf{C}_m(\mathbf{b}(t)) = -\left[\mathbf{b}(t)\times\right]\mathbf{G}, \tag{5}$$

where $\mathbf{G} \in \mathbb{R}^{3\times l}$ is a static geometric distribution matrix of moments. The negative sign for $\mathbf{C}_w$ represents the reactive torque required for an internally actuated system. The matrices $\mathbf{C}_w$ and $\mathbf{C}_T$ are also assumed to be static.

3. CONSTRAINED CONTROL ALLOCATION

3.1 Problem Statement

The main function of the magnetorquers is to slowly dump momentum built up in the reaction wheels due to secular external disturbance torques, which can be crucial for reaction wheel system performance as the wheel speed $\boldsymbol{\omega}_w$ is otherwise prone to dead-zone crossings and saturation. Thrusters may provide faster momentum dumping and do not rely on an external magnetic field to do so. A virtual hybrid momentum dumping control law to handle this is given by a variant of that found in (Markley and Crassidis, 2014),

$$\mathbf{u}_h = -k_h\left(\mathbf{I}_3 - \theta\hat{\mathbf{b}}\hat{\mathbf{b}}^\intercal\right)\mathbf{C}_w\mathbf{J}_w\boldsymbol{\omega}_{w,e}, \tag{6}$$

where $\mathbf{J}_w \in \mathbb{R}^{3\times3}$ is the inertia matrix of the reaction wheels about their spin axes; $\boldsymbol{\omega}_{w,e} = \boldsymbol{\omega}_w - \boldsymbol{\omega}_{w,d}$ is the wheel speed error with $\boldsymbol{\omega}_w \in \mathbb{R}^3$ being the measured/estimated wheel speed and $\boldsymbol{\omega}_{w,d} \in \mathbb{R}^3$ is the wheel speed reference; and $k_h = \theta k_m + (\rho-\theta)k_T \in \mathbb{R}$ with positive constants $k_m > 0 \in \mathbb{R}$ set to be relatively small to accommodate the saturation limits of the magnetic moments, and $k_T > k_m \in \mathbb{R}$ is greater if using thrusters is applicable and momentum dumping must happen faster; and $1 \le \rho \le 2 \in \mathbb{R}$. If $\rho > 1$ while $\theta = 1$, then the thrusters work together with magnetorquers. The allocation of $\mathbf{u}_h$ to available actuators that produce external torques can be written as

$$\mathbf{u}_h(t) = \theta\mathbf{C}_m(t)\mathbf{m}(t) + (\rho-\theta)\mathbf{C}_T\boldsymbol{\tau}_T(t) = \boldsymbol{\tau}_h(t). \tag{7}$$

The CA problem may have mixed optimization objectives for minimizing the error between the commanded input $\mathbf{u}$ and the provided torque $\boldsymbol{\tau}$ in the body frame, while minimizing the control effort and/or power consumption. Also accommodating the control in (7) as an objective, the problem can be written as

$$\min_{\boldsymbol{\tau}_a\in\mathcal{T}_a} \quad \frac{1}{2}\boldsymbol{\tau}_a^\intercal\mathbf{W}(t)\boldsymbol{\tau}_a + \frac{1}{2}\mathbf{s}^\intercal\mathbf{V}\mathbf{s}, \tag{8a}$$

$$\text{s.t.} \quad \mathbf{C}\boldsymbol{\tau}_a = \mathbf{u} + \mathbf{s}_1, \tag{8b}$$

$$\theta\mathbf{C}_m\mathbf{m} + (\rho-\theta)\mathbf{C}_T\boldsymbol{\tau}_T = \mathbf{u}_h + \mathbf{s}_2, \tag{8c}$$

where $\mathbf{W}(t) \in \mathbb{R}^{p\times p}$ is taken to be a dynamic diagonal weight matrix that may favor groups or individual actuators; $\mathbf{s} = [\mathbf{s}_1^\intercal, \mathbf{s}_2^\intercal]^\intercal$ with $\mathbf{s}_1 \in \mathbb{R}^3$ and $\mathbf{s}_2 \in \mathbb{R}^3$, is a slack variable; and $\mathbf{V} = \text{diag}(\mathbf{V}_1, \mathbf{V}_2) \in \mathbb{R}^{6\times6}$ is a constant block-diagonal weight matrix for prioritizing the equality constraints (8b) and (8c), where $\mathbf{V}_1 = v_1\mathbf{I}_3$ and $\mathbf{V}_2 = v_2\mathbf{I}_3$. The constants v_2 may be set slightly lower than v_1 if the main objective is attitude control, and vice versa.

The minimization problem (8a)-(8c) can be implemented in a convex QP form as

$$\min_{\boldsymbol{\tau}_a,\mathbf{s}} \quad \frac{1}{2}\mathbf{z}^\intercal\mathbf{H}\mathbf{z}, \tag{9a}$$

$$\text{s.t.} \quad \begin{bmatrix}-\mathbf{I}_p, & \mathbf{0}_{p\times6}\\ \mathbf{I}_p, & \mathbf{0}_{p\times6}\end{bmatrix}\mathbf{z} \le \begin{bmatrix}-\underline{\boldsymbol{\tau}}_a\\ \overline{\boldsymbol{\tau}}_a\end{bmatrix}, \tag{9b}$$

$$\begin{bmatrix}\mathbf{C}_w, & \theta\mathbf{C}_m(t), & \mathbf{C}_T, & -\mathbf{I}_3, & \mathbf{0}_{3\times3}\\ \mathbf{0}_{3\times m}, & \theta\mathbf{C}_m(t), & (\rho-\theta)\mathbf{C}_T, & \mathbf{0}_{3\times3}, & -\mathbf{I}_3\end{bmatrix}\mathbf{z} = \begin{bmatrix}\mathbf{u}\\ \mathbf{u}_h\end{bmatrix}, \tag{9c}$$

where $\mathbf{z} \triangleq [\boldsymbol{\tau}_a^\intercal, \mathbf{s}^\intercal]^\intercal \in \mathbb{R}^{p+6}$, and $\mathbf{H} \in \mathbb{R}^{(p+6)\times(p+6)}$ is a positive definite diagonal matrix $\mathbf{H} \triangleq 2\cdot\text{diag}(\mathbf{W}(t), \mathbf{V})$. The QP method provides solutions that demand torques from all actuators in general, in contrary to linear programming which in essence completely avoids using actuators that have large weights (Bodson, 2002). When $\theta = 0$, an option is to remove $\mathbf{C}_m$ from (3) to improve the computational speed in finding a solution.

3.2 Dynamic Weighting

For equally sized reaction wheels being the main actuators for attitude control, the weights are set to $\mathbf{W}_w = \text{diag}(\mathrm{w}_{w,1}, \mathrm{w}_{w,2}, \dots \mathrm{w}_{w,r}) = \eta_w\mathbf{I}_r$. The other weights $\mathbf{W}_m(t) = \text{diag}(\mathrm{w}_{m,1}(t), \mathrm{w}_{m,2}(t), \dots \mathrm{w}_{m,l}(t)) = \eta_m(t)\mathbf{I}_l$ and $\mathbf{W}_T(t) = \text{diag}(\mathrm{w}_{T,1}(t), \mathrm{w}_{T,2}(t), \dots \mathrm{w}_{T,k}(t)) = \eta_T(t)\mathbf{I}_k$ for slower and faster actuators, respectively, can then be designed *relative* to those in $\mathbf{W}_w$. Without loss of generality, the parameter η_w can be set to $\eta_w = 1$.

The weight parameters for magnetorquers can be defined as a bounded function $0 < \eta_m(t) \le K_L$ for a constant $K_L > 0 \in \mathbb{R}$,

$$\eta_m(t) = \frac{\eta_w\left(1 + \theta e^{b_0/(\|\mathbf{b}(t)\|+\gamma_2)}\right)}{\gamma_1 + \theta\left(\alpha_1 z_1(t) + \alpha_2 z_2(t)\right)}, \tag{10}$$

where $z_1 = \|\boldsymbol{\omega}_{w,e}\|$, $z_2 = \|\mathbf{q}_{v,e} + \kappa\boldsymbol{\omega}_e\|$; $b_0 > 0 \in \mathbb{R}$ is a nominal magnetic field strength; $\alpha_1 \ge 0 \in \mathbb{R}$, $\alpha_2 \ge 0 \in \mathbb{R}$, $\kappa \ge 0 \in \mathbb{R}$ determine the relative importance of using magnetorquers for momentum dumping versus attitude control; and $\gamma_1 > 0 \in \mathbb{R}$ and $\gamma_2 > 0 \in \mathbb{R}$ are regularization terms to avoid division by zero. The shape of this function is shown in Figure 2. If tuning the denominator in (10) to be small or if the magnetic field is sufficiently weak, i.e. shown in Figure 3, then usage of magnetorquers will be heavily penalized. This may be favored during slow attitude control with smaller reaction wheel torques, where usage of magnetorquers may be unneccessary or even inconvenient. The proposed dynamic weight in (10) and other variants can, with careful tuning, be useful for highly elliptical orbits and orbit maneuvers to higher/lower altitudes, where continuous functions may be favoured over on-off switching with boolean logic. Alternative time-varying weighting function can also be based on a variant of the logistic equation for population growth, e.g. see (Hu and Tan, 2020) for a variant of weighting CMGs that includes penalty on approaching their geometric singularity.

Using similar logic as for magnetorquers, the weights for the thrusters can be defined as

$$\eta_T(t) = \frac{\eta_w}{\gamma_3 + \beta_1(\rho-\theta)z_1(t) + \beta_2 z_2(t)}, \tag{11}$$

where $\beta_1 \ge 0 \in \mathbb{R}$, $\beta_2 \ge 0 \in \mathbb{R}$, and $\gamma_3 > 0 \in \mathbb{R}$, and the regularization term γ_3 should be taken to be much smaller than γ_1 if saving fuel/power is desired.

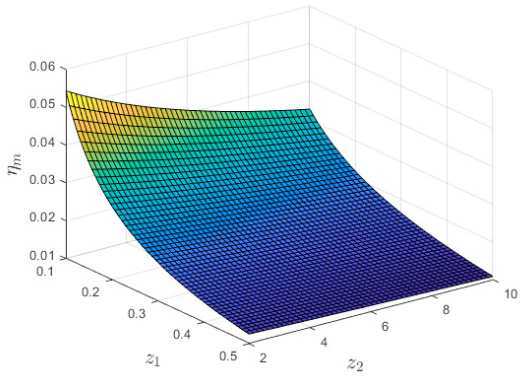

Fig. 2. A cut-out for η_m versus z_1 and z_2 for $b_0 = 2\times10^{-5}$, $\|\mathbf{b}\| = 2.45 \times 10^{-5}$, $\alpha_1 = 5$, $\alpha_2 = 500$, $\kappa = 0.1$, $\gamma_1 = 0.01$, and $\gamma_2 = 1 \times 10^{-7}$.

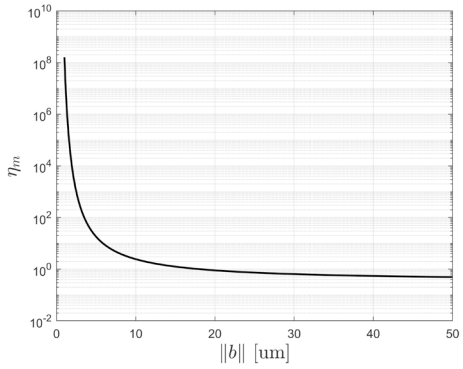

Fig. 3. Weight parameter η_m on a logarithm scale versus magnetic field strength $\|\mathbf{b}\|$ for $z_1 = 0.1$, $z_2 = 0.005$, $b_0 = 2 \times 10^{-5}$, $\alpha_1 = 5$, $\alpha_2 = 500$, $\kappa = 0.1$, $\gamma_1 = 0.01$, and $\gamma_2 = 1 \times 10^{-7}$.

4. SIMULATIONS

The total spacecraft inertia matrix is chosen as

$$\mathbf{J} = \begin{bmatrix} 0.0775 & 0.0005 & -0.0002 \\ -0.0005 & 0.1067 & 0.0002 \\ 0.0002 & -0.0002 & 0.0389 \end{bmatrix} \text{kgm}^2, \tag{12}$$

We consider $r = 4$ reaction wheels with inertia matrix $\mathbf{J}_w = 2.3 \times 10^{-5} \cdot \mathbf{I}_4\,\text{kgm}^2$ and distribution matrix,

$$\mathbf{C}_w = \begin{bmatrix} 1 & 0 & 0 & 1/\sqrt{3} \\ 0 & 1 & 0 & 1/\sqrt{3} \\ 0 & 0 & 1 & 1/\sqrt{3} \end{bmatrix}. \tag{13}$$

Since $\text{rank}(\mathbf{C}_w) = 3 < 4$, the reference wheel speed vector is chosen as,

$$\boldsymbol{\omega}_{w,d} = 2000 \cdot \left[1,\ 1,\ 1,\ -\sqrt{3}\right]^\intercal \text{ rpm}, \tag{14}$$

which belongs to the nullspace $\ker(\mathbf{C}_w)$.

Furthermore, it is assumed that there are two thrusters ($k = 2$) that are perfectly coupled and mounted on the largest sides of the spacecraft with distribution matrix,

$$\mathbf{C}_T = \begin{bmatrix} 0 & 0 \\ 1 & -1 \\ 0 & 0 \end{bmatrix}. \tag{15}$$

The number of magnetorquers are chosen such that they are mounted along each body axis and provide moments either direction ($l = 6$), with distribution matrix set to,

$$\mathbf{G} = [\mathbf{I}_3,\ -\mathbf{I}_3]\,. \tag{16}$$

To simulate the dynamics (1a) and (1b) in a realistic setting, the disturbance torques in $\mathbf{d}$ are modelled based on (Markley and Crassidis, 2014) with parameters used in (Grøtte et al., 2020), including distrubances from spacecraft magnetic dipole, solar radiation pressure, atmospheric drag, and gravity gradient. The initial orbit parameters were set to a semi-major axis of 6871 km assuming the Earth as the primary body, eccentricity of 1×10^{-5}, inclination of 97.6 deg, Right-Ascension of Ascending Node of 80 deg, argument of periapsis of 0 deg, and true anomaly of 0 deg. The geomagnetic field strength $\mathbf{b}$ is computed using the IGRF-13 model at epoch t_0 of 10 July 2023 00:00:00. Simulation time is set to 60 s and the dynamics are numerically integrated using forward Euler method with a timestep of 0.1 s. The CA was solved at each time instant using *quadprog* in the Matlab 2021b Optimization Toolbox with an average computation time of 0.0058 s on a HP laptop computer with Intel Core i5 processor running Windows 11.

The initial conditions in the simulations are set to $\mathbf{q}(t_0) = [0.711,\ 0.319,\ -0.283,\ 0.559]^\intercal$, and $\boldsymbol{\omega}(t_0) = [0,\ -0.00111,\ 0]^\intercal$, and $\boldsymbol{\omega}_w(t_0) = \boldsymbol{\omega}_{w,d}$. The second element of $\boldsymbol{\omega}(t_0)$ corresponds to the orbit angular velocity. Desired states are $\mathbf{q}_d(t_0) = [-0.340,\ -0.610,\ 0.686,\ -0.203]^\intercal$ and angular velocity $\boldsymbol{\omega}_d = [0,\ -0.00111,\ 0]^\intercal$, corresponding to a rotation from 40 deg to −40 deg about the y-axis of the body frame with respect to nadir, i.e., a desired change of principal angle of $\Phi_e(t_0) \triangleq 2\cos^{-1}(\mathbf{q}_{0,e}(t_0)) = -80$ deg.

The chosen attitude control law for $\mathbf{u}$ is a proportional-derivative controller (Wie and Barba, 1985) that almost globally asymptotically stabilizes the system in Eqs. (1a) and (1b),

$$\mathbf{u} = -k_p \text{sign}(q_{0,e})\mathbf{q}_{v,e} - k_d\boldsymbol{\omega}_e, \tag{17}$$

where $k_p > 0 \in \mathbb{R}$, $k_d > 0 \in \mathbb{R}$, and

$$\text{sign}(q_{0,e}) = \begin{cases} 1, & q_{0,e} \geq 0, \\ -1, & q_{0,e} < 0, \end{cases} \tag{18}$$

Given the initial and desired states used, the constants are chosen as $k_p = 2 \times 10^{-2}$ and $k_d = 8 \times 10^{-2}$ for fast maneuvers, and $k_p = 3.5 \times 10^{-3}$ and $k_d = 1 \times 10^{-2}$ for slow maneuvers. The attitude and angular velocity errors are shown in Figure 4 for the fast maneuver, settling to approximately zero around $t = 30$ s. The same is shown in Figure 5 but for a slower maneuver with twice the settling time at around $t = 60$ s.

To illustrate the results using the CA scheme in (9a), (9b), and (9c), and dynamic weighting using (10) and (11), the following cases are investigated for aforementioned initial conditions, desired conditions, control law gains, and the parameters in Table 1,

- Case 1: Fast attitude control where only magnetorquers are used for momentum dumping ($\rho = 1$ and $\theta = 1$).
- Case 2: Fast attitude control where both thrusters and magnetorquers are used for momentum dumping ($\rho = 2$ and $\theta = 1$).

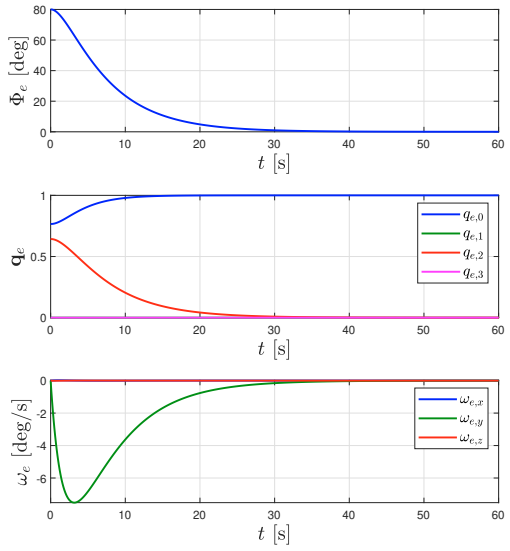

Fig. 4. Principal angle, quaternion and angular velocity errors for Case 1.

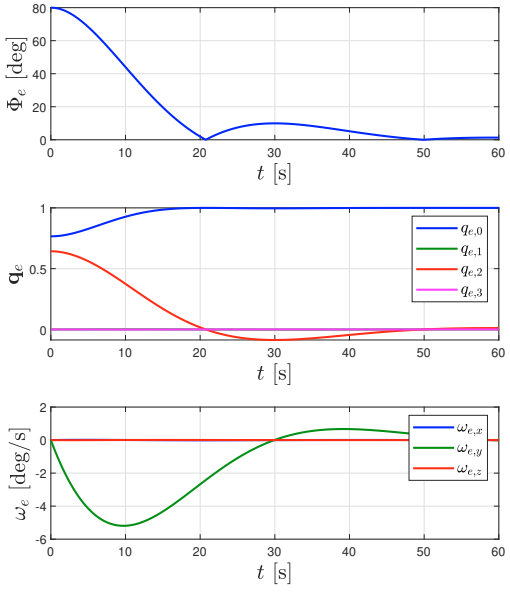

Fig. 5. Principal angle, quaternion and angular velocity errors for Case 3.

- Case 3: Slow attitude control where only magnetorquers are used for momentum dumping ($\rho = 1$ and $\theta = 1$).

4.1 Case 1

The fast rotation causes all reaction wheel torques to saturate as seen in Figure 6, demanding that magnetorquers and one thruster must provide aid so that the constraint (2) is satisfied during the steep angular acceleration $\dot{\boldsymbol{\omega}}$ in the first seconds. Figure 7 shows that the constraint (2) is satisfied in the x, y and z directions in the body frame for desired control $\mathbf{u}$ (dashed) and actual control $\boldsymbol{\tau}$ (solid).

Table 1. Simulation parameters

Parameter	Value
$\overline{\tau}_w$	3.2×10^{-3} Nm
$\overline{\tau}_T$	0.05 Nm
$\overline{m}$	0.92 Am^2
$\underline{\tau}_w$	-3.2×10^{-3} Nm
$\underline{\tau}_T$	0 Nm
$\underline{m}$	0 Am^2
k_m	2×10^{-3}
k_T	0.5
η_w	1
ϵ	1×10^{-7} T
b_0	2.45×10^{-5} T
γ_1	1×10^{-2}
γ_2	1×10^{-7}
α_1	20
α_2	1×10^{5}
κ	0.1
γ_3	1×10^{-6}
β_1	1×10^{-5}
β_2	1×10^{-5}
v_1	2×10^{7}
v_2	1×10^{7}

A small deviation can be seen in $\boldsymbol{\tau}_h$ versus $\mathbf{u}_h$ (middle) in the first seconds as the magnetorquers are helping the reaction wheels in attitude control before engaging only in momentum dumping to satisfy (7). The second reaction wheel speed approaches close to zero, meaning it is prone to crossing the dead-zone and it takes a long time for the momentum to be unloaded by the magnetorquers. Figure 8 shows the weighting parameters η_m and η_T, increasing noticeably when attitude error becomes smaller.

Using static weights $\eta_m = 0.1$ and $\eta_T = 1 \times 10^5$ instead of the dynamic ones using (10) and (11), then Figures (9) and (10) show that both magnetorquers and thrusters contribute to attitude control, but the magnetorquers are barely used for momentum dumping and control allocation in (7) is not satisfied.

4.2 Case 2

Performing a fast maneuver and also faster momentum dumping with both magnetorquers and thrusters achieves similar performance to Case 1 in minimizing both $\boldsymbol{\tau} - \mathbf{u}$ and $\boldsymbol{\tau}_h - \mathbf{u}_h$, seen in Figure 11, however it can be seen that the settling time for reaction wheel speed is shorter and therefore the wheel momenta are dumped much quicker because one thruster accelerates and another one brakes the system as seen in Figure 12. Although with fairly small magnetic torques, the magnetorquers also aid in this case with higher moments than in Case 1 since they are still prioritized but they quickly settle down [2]. Figure 13 shows the weighting parameters η_m and η_T, where the latter continues to be weighted since the thrusters should be available for momentum dumping.

4.3 Case 3

Sufficiently slow attitude control and slow momentum dumping do not cause reaction wheels nor magnetorquers

[2] When $\theta = 0$, although not shown here, the CA scheme would not demand any control effort from magnetorquers and similar results can be expected as for using both thrusters and magnetorquers.

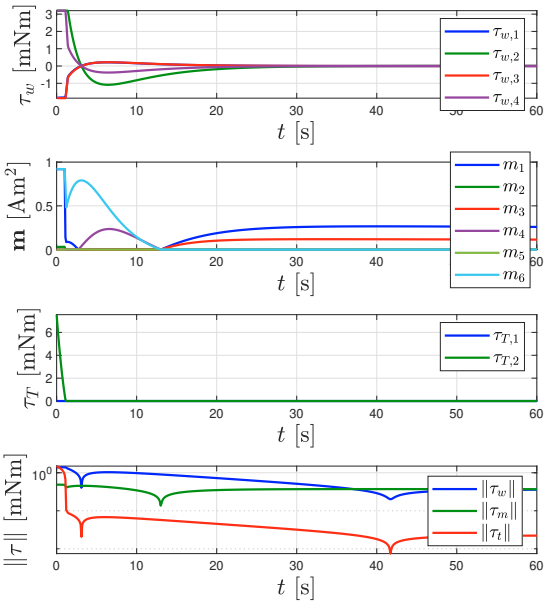

Fig. 6. Reaction wheel torques, magnetorquer moments, thruster torques and the norm of torques of each type for Case 1.

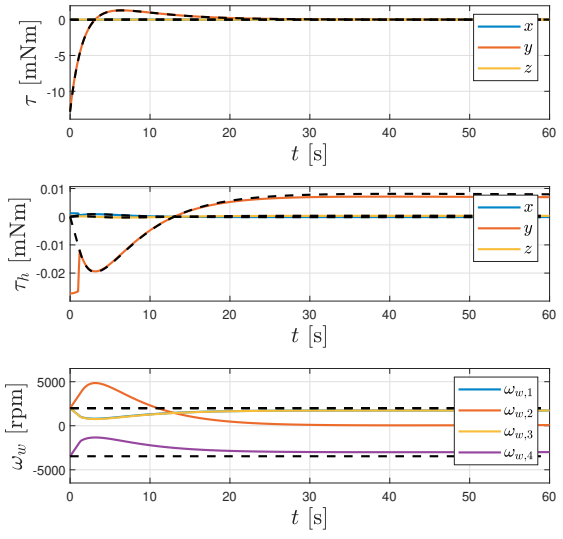

Fig. 7. Virtual controls $\mathbf{u}$ and $\mathbf{u}_h$ (dashed) and control input obtained from CA (solid) for Case 1.

to saturate, and thrusters are not needed at all. Figure 14 shows that the control errors are small, i.e. (2) and (7) are practically satisfied, and that the reaction wheel speed stay away from zero-crossing and settle down close to the reference. Figure 15 shows the reaction wheels and magnetorquers running without saturating, and the demanded thruster torques are negligible. Figure 16 shows the weighting parameters η_m and η_T increasing with smaller attitude control error.

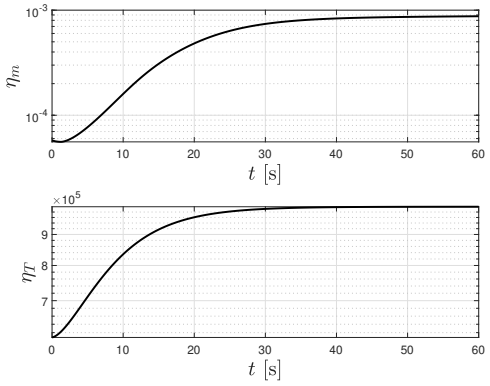

Fig. 8. Weight parameters η_m and η_T versus time t for Case 1.

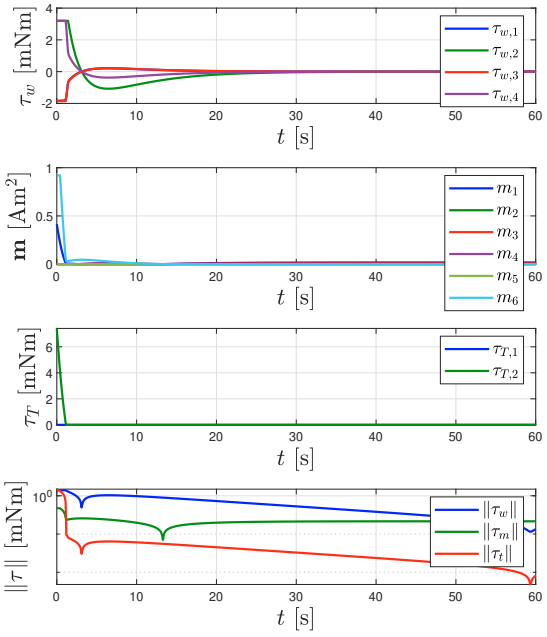

Fig. 9. Reaction wheel torques, magnetorquer moments, thruster torques and the norm of torques of each type for Case 1 but with static weights.

5. CONCLUSIONS

Mixed optimization in control allocation has been investigated for a spacecraft attitude control problem using a hybrid assembly of reaction wheels, thrusters and magnetorquers. Quadratic programming minimizes the least-squares error and utilizes all actuators to some degree. For high-torque profiles, the dynamic weights in control allocation provides additional flexibility for tuning the distribution of control effort for slow, medium and fast actuators. A second equality constraint has been defined in the CA optimization to allow for satisfying desired momentum dumping of reaction wheels. Future work will investigate the inclusion of deadzone constraints.

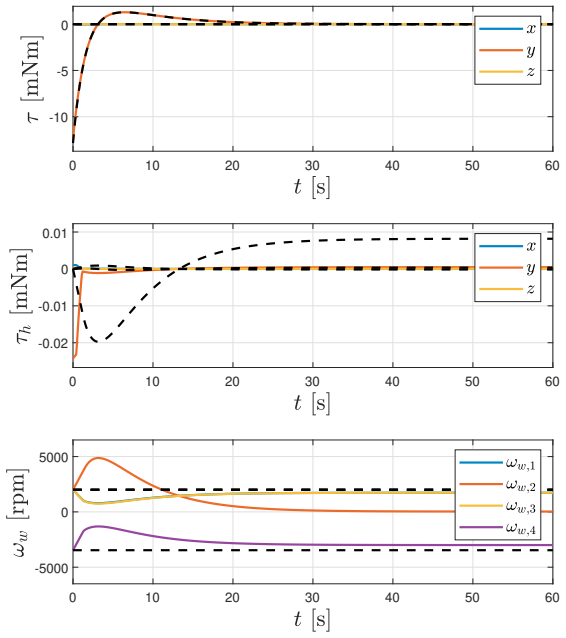

Fig. 10. Virtual controls $\mathbf{u}$ and $\mathbf{u}_h$ (dashed) and control input obtained from CA (solid) for Case 1 but with static weights.

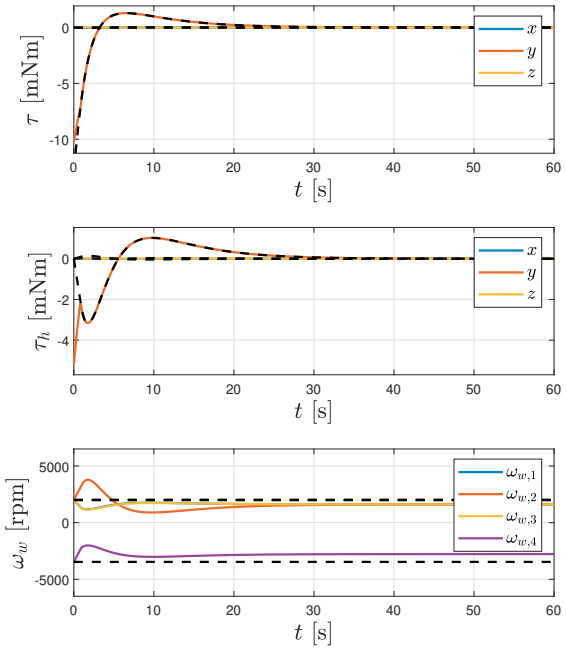

Fig. 11. Virtual controls $\mathbf{u}$ and $\mathbf{u}_h$ (dashed) and control input obtained from CA (solid) for Case 2.

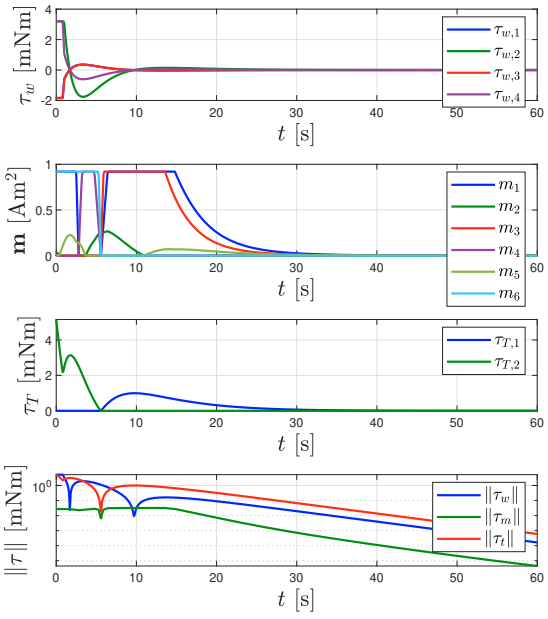

Fig. 12. Reaction wheel torques, magnetorquer moments, thruster torques and the norm of torques of each type for Case 2.

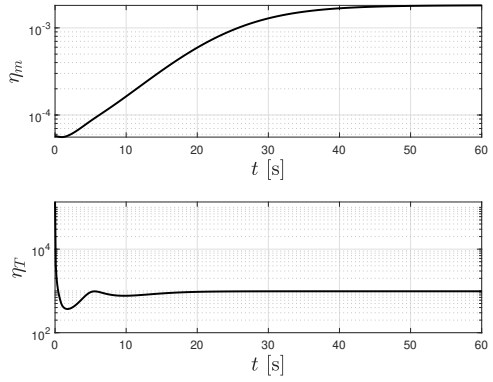

Fig. 13. Weight parameters η_m and η_T versus time t for Case 2.

REFERENCES

Bilimoria, K.D. and Wie, B. (1993). Time-optimal three-axis reorientation of a rigid spacecraft. *Journal of Guidance, Control, and Dynamics*, 16(3), 446–452.

Bodson, M. (2002). Evaluation of optimization methods for control allocation. *Journal of Guidance, Control, and Dynamics*, 25(4), 703–711.

Cristofaro, A. and Johansen, T.A. (2014). Fault tolerant control allocation using unknown input observers. *Automatica*, 50(7), 1891–1897.

Fleming, A., Sekhavat, P., and Ross, I.M. (2010). Minimum-time reorientation of a rigid body. *Journal of Guidance, Control, and Dynamics*, 33(1), 160–170.

Grøtte, M.E., Gravdahl, J.T., Johansen, T.A., Larsen, J.A., Vidal, E.M., and Surma, E. (2020). Spacecraft attitude and angular rate tracking using reaction wheels and magnetorquers. *IFAC-PapersOnLine*, 53(2), 14819–

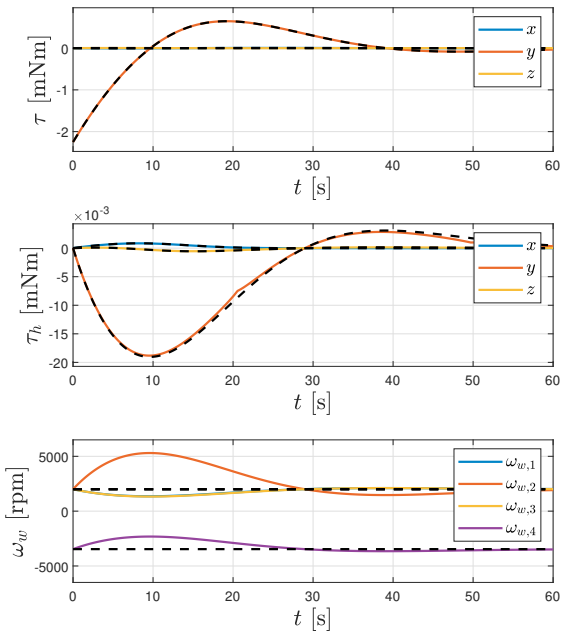

Fig. 14. Virtual controls $\mathbf{u}$ and $\mathbf{u}_h$ (dashed) and control input obtained from CA (solid) for Case 3.

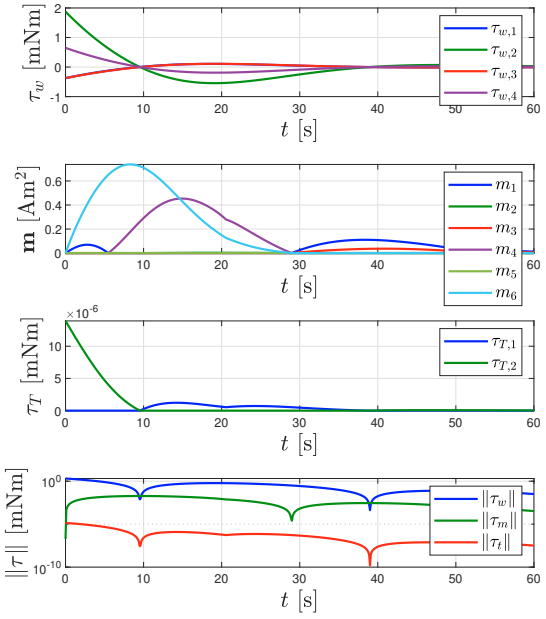

Fig. 15. Reaction wheel torques, magnetorquer moments, thruster torques and the norm of torques of each type for Case 3.

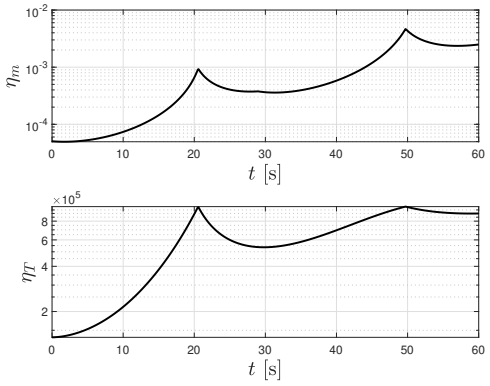

Fig. 16. Weight parameters η_m and η_T versus time t for Case 3.

14826. 21st IFAC World Congress.

Harkegard, O. (2002). Efficient active set algorithms for solving constrained least squares problems in aircraft control allocation. In *Proceedings of the 41st IEEE Conference on Decision and Control, 2002.*, volume 2, 1295–1300 vol.2.

Hu, Q. and Tan, X. (2020). Dynamic near-optimal control allocation for spacecraft attitude control using a hybrid configuration of actuators. *IEEE Transactions on Aerospace and Electronic Systems*, 56(2), 1430–1443.

Hu, Q., Tan, X., and Akella, M.R. (2018). Closed-loop-based control allocation for spacecraft attitude stabilization with actuator fault. *Journal of Guidance, Control, and Dynamics*, 41(4), 944–953.

Johansen, T.A. and Fossen, T.I. (2013). Control allocation—a survey. *Automatica*, 49(5), 1087–1103.

Leeghim, H. and Kim, D. (2021). Singularity-robust control moment gyro allocation strategy for spacecraft attitude control in the presence of disturbances. *Aerospace Science and Technology*, 119, 107178.

Liu, S.W. and Singh, T. (1997). Fuel/time optimal control of spacecraft maneuvers. *Journal of Guidance, Control, and Dynamics*, 20(2), 394–397.

Markley, L. and Crassidis, J. (2014). *Fundamentals of Spacecraft Attitude Determination and Control*.

Melton, R.G. (2014). Hybrid methods for determining time-optimal, constrained spacecraft reorientation maneuvers. *Acta Astronautica*, 94(1), 294–301.

Oppenheimer, M.W., Doman, D.B., and Bolender, M.A. (2006). Control allocation for over-actuated systems. In *2006 14th Mediterranean Conference on Control and Automation*, 1–6.

Scrivener, S.L. and Thompson, R.C. (1994). Survey of time-optimal attitude maneuvers. *Journal of Guidance, Control, and Dynamics*, 17(2), 225–233.

Seywald, H., Kumar, R.R., Deshpande, S.S., and Heck, M.L. (1994). Minimum fuel spacecraft reorientation. *Journal of Guidance, Control, and Dynamics*, 17(1), 21–29.

Sin, E., Arcak, M., Nag, S., Ravindra, V., Li, A., and Levinson, R. (2021). *Attitude Trajectory Optimization for Agile Satellites in Autonomous Remote Sensing Constellations*, 1–19.

Steyn, W.H. (1995). Near-minimum-time eigenaxis rotation maneuvers using reaction wheels. *Journal of Guidance, Control, and Dynamics*, 18(5), 1184–1189.

Wie, B. and Barba, P.M. (1985). Quaternion feedback for spacecraft large angle maneuvers. *Journal of Guidance, Control, and Dynamics*, 8(3), 360–365.